# Reconstructing structural changes in a dynamic system
# from experimentally identified state-space models

B. H. Koh[1,*], S. Nagarajaiah[2] and M. Q. Phan[3]

[1]*Assistant Professor, Department of Mechanical Engineering, Dongguk University, 3-26 Pil-dong, Chung-gu, Seoul 100-715, Korea*
[2]*Professor, Department of Civil and Environmental Engineering Department of Mechanical
Engineering and Material Science, Rice University, Houston, TX 77005, USA*
[3]*Associate Professor, Thayer School of Engineering, Dartmouth College, Hanover, NH 03755, USA*

---

## Abstract

This paper presents an experimental investigation of a recently developed Kronecker Product (KP) method to determine the type, location, and intensity of structural change from an identified state-space model of the system. Although this inverse problem appears to be highly nonlinear, the system mass, stiffness, and damping matrices are identified through a series of transformations, and with the aid of the Kronecker product, only linear operations are involved in the process. Since a state-space model can be identified directly from input-output data, an initial finite element model and/or model updating is not required. The test structure is a two-degree-of-freedom torsional system in which mass and stiffness are arbitrarily adjustable to simulate various conditions of structural change or damage. This simple apparatus illustrates the potential applicability of the system identification technique for damage detection problems by not only identifying the location and the extent of the damage, but also differentiating the nature of the damage. The results are successfully confirmed by laboratory tests.

*Keywords*: Kronecker product; State-space model; Structural damage; System identification

---

## 1. Introduction

Identifying structural parameters from input-output data has been widely investigated for developing reliable and cost-effective tools in monitoring the condition of structures. One of major difficulties in structural damage detection using vibration signatures, such as natural frequencies, mode shapes, and frequency response function, is that the approach is inherently model-based [1]. In other words, damage-sensitive parameters of the structure have to be measured and assessed before and after the occurrence of damage. Many of the damage detection methods, however, simply presume that a reference (undamaged) model is already known with sufficient accuracy. If that is not the case, the reference model has to

be validated through various model updating techniques to fully represent the true state of an undamaged system [2]. Typical model updating methods require a prototype of a finite element model before initiating its tuning process. Developing a prototype model and improving its fidelity is already a challenging task because the effect of modeling errors between the original model and true structure quite often far exceeds the difference caused by damage itself [3,4]. Moreover, in most cases separating these errors from structural damages is not straightforward [5]. This severe gap between initial model and true structure limits the performance of many damage detection techniques in the field. Thus, the dependence on initial finite element models should be minimized to improve the detectability of a damage detection method. If we can reconstruct the second-order model of a mechanical system such as mass, stiffness, and

---
*Corresponding author. Tel.: +82 2 2260 8591, Fax.: +82 2 2263 9379
E-mail address: bkoh@dongguk.edu

damping matrices directly from input-output data, the necessity of a prototype model and its tuning process can be simultaneously avoided or reduced.

The research on the realization of state-space model from input-output data has been well developed for the last few decades. A standard system identification algorithm such as OKID-ERA [6, 7] determines a minimally realized state-space model from observer Markov parameters and truncation of a Hankel matrix. However rearranging a state-space model into a second-order form such as mass, stiffness, and damping matrices is non-trivial because typically a realized state-space model is not in physical coordinates. There have been several research efforts trying to extract second-order mechanical system matrices from identified state-space models. Alvin and Park [8] developed a transformation algorithm using the McMillan normal form realization. The study also includes other variants of the method that can estimate normal mode from non-proportional damping through pseudo-normal mode basis. Tseng et al. [9] investigated an algorithm that can also deal with gyroscopic systems with repeated undamped modal frequencies. Angelis et al. [10] proposed a more generalized technique that relaxes the constraints on the number of sensors/actuator and co-location requirements. However, all of these studies need an intermediate nonlinear step of solving eigenvalue problems. Recently, Phan and Longman [11] developed a linear solution for extracting system parameters in physical coordinates via the properties of Kronecker product and stack operation. First, a state-space model is identified from input-output data by any state-space system identification technique such as OKID-ERA. From such an identified state-space model, structural properties, i.e., stiffness, mass, and damping matrices can be extracted from a series of linear transformations. Previously, Ray and Koh [12] investigated a damage detection problem in torsional systems, given the empirical correlation between feedback control gain and sensitivity of modal frequencies. Experimental results proved that the modal sensitivity of structural damage in torsional system could be significantly enhanced through sensitivity enhancing control (SEC). However, their approach, like all other modal-based damage detection methods, requires information of modal frequencies of the test structure. Modal frequency is a global property of dynamic system and sensitive to both mass and stiffness variations. In general, observation of modal frequency change alone

is insufficient for identifying the type of damage (i.e., mass or stiffness).

This paper presents an experimental verification of the Kronecker Product (KP) method [11]. However, the focus is on whether the technique can be practically applied to damage detection problems by comparing the reconstructed structural parameters such as mass and stiffness before and after the occurrence of damage. The strength of this approach compared to other modal-based methods lies in a successful identification of damage presence, location, and type, without any prior knowledge of the FE model of the structure. First, the mathematical formulation of KP method is briefly explained. Second, the experimental procedure and test setup are described. The test-bed in this study is a two-degree-of-freedom torsional system. The proposed approach does not require modal frequencies or a baseline finite element model. To introduce different types of damage conditions, the mass and stiffness of the system are systematically perturbed. Finally, test results are presented and discussed in terms of damage localization and classification of damage type. This experimental demonstration should be considered as a preliminary step in a series of efforts for implementing a system identification algorithm into the development of structural damage detection technique for more complicated structures. The same experiment data, i.e., input-output time history of the torsional system in reference [12] is used in this study.

## 2. Kronecker product method

Although the reference [11] provides a detailed derivation of the KP method, for the sake of completeness, a brief summary is provided for the case of having a full set of displacement measurement in this section. Consider a spatially discrete system having $n$ physical coordinates $w(t)$ and $r$ inputs $u(t)$

$$\mathsf{M}\ddot{w}(t) + \Theta\dot{w}(t) + \mathsf{K}w(t) = \mathsf{B}u(t) \quad (1)$$

where $\mathsf{M}$, $\Theta$, and $\mathsf{K}$ are mass, damping, and stiffness matrices, respectively. The $\mathsf{B}$ ($n \times r$) is the input influence matrix. The second-order equation of motion can be rewritten in a state-space format with its physical coordinates intact as

$$\begin{aligned} \dot{x}(t) &= Ax(t) + Bu(t) \\ y(t) &= Cx(t) + Du(t) \end{aligned} \quad (2)$$

$$x(t) = \begin{bmatrix} w(t) \\ \dot{w}(t) \end{bmatrix}, \quad A = \begin{bmatrix} 0_{n \times n} & I_{n \times n} \\ -H_1 & -H_2 \end{bmatrix}, \quad B = \begin{bmatrix} 0_{n \times r} \\ H_3 \end{bmatrix} \quad (3)$$

Here, partitions holding $M$, $\Theta$, and $K$ can be expressed as

$$H_1 = M^{-1}K, \qquad H_2 = M^{-1}\Theta, \qquad H_3 = M^{-1}B. \quad (4)$$

If we have a full set of displacement measurements (which is the case for this experiment),

$$C = \begin{bmatrix} I_{n \times n} & 0_{n \times n} \end{bmatrix}, \quad D = 0_{n \times r} \quad (5)$$

Given $H_{i=1...3}$ in physical coordinates, structural parameters $M$, $\Theta$, and $K$ can be extracted from the Kronecker product and stack operator techniques presented in Section 2.2.

### 2.1 Transforming physical coordinates

Unfortunately, a realized state-space model is not necessarily in the physical coordinates given in Eq. (3) and (4). Then the first step in extracting $M$, $\Theta$, $K$ is to transform a realized state-space model into a physical coordinate system. Here a transformation matrix is developed that will transform any realized state-space model $(A_r, B_r, C_r)$ into the physical coordinates of $(A, B, C)$. We review the case where a full set of displacement measurements is available. Other cases for velocity, acceleration, and mixed measurements are explained in the reference [11]. In deriving this transformation matrix, a similarity transformation matrix $Q$ is used.

$$\begin{aligned} \tilde{A} &= Q(A_r)Q^{-1} \\ \tilde{B} &= Q(B_r) \\ \tilde{C} &= (C_r)Q^{-1} = \begin{bmatrix} I_{n \times n} & 0_{n \times n} \end{bmatrix} = C \end{aligned} \quad (6)$$

where,

$$Q = \begin{bmatrix} C_r \\ \hline \bar{Q} \end{bmatrix} \quad (7)$$

here, $\bar{Q}$ is any nonsingular matrix. This intermediate step is purely to transform $C_r$ into $C$. Another similarity transformation $T$ is needed to transform $(\tilde{A}, \tilde{B})$ into $(A, B)$ without modifying $C$ which is already transformed correctly by $Q$. Accordingly,

the transformation matrix $T$ should satisfy

$$\begin{aligned} A &= T(\tilde{A})T^{-1} \\ B &= T(\tilde{B}) \\ \tilde{C} &= (\tilde{C})T^{-1} \end{aligned} \quad (8)$$

For further development, $T$, $A$, $\tilde{A}$, and $B$ are partitioned as

$$T = \begin{bmatrix} T_{11} & T_{12} \\ T_{21} & T_{22} \end{bmatrix}, \quad A = \begin{bmatrix} 0 & I \\ A_{21} & A_{22} \end{bmatrix},$$
$$\tilde{A} = \begin{bmatrix} (\tilde{A})_{11} & (\tilde{A})_{12} \\ (\tilde{A})_{21} & (\tilde{A})_{22} \end{bmatrix}, \quad B = \begin{bmatrix} B_1 \\ B_2 \end{bmatrix} \quad (9)$$

Note that the transformed matrices $(\tilde{A}, \tilde{B})$ belong to an intermediate step between a realized state-space model and a state-space model in physical coordinates. Here, another condition is imposed to $T$ that will preserve $\tilde{C}$,

$$\begin{bmatrix} I & 0 \end{bmatrix} \begin{bmatrix} T_{11} & T_{12} \\ T_{21} & T_{22} \end{bmatrix} = \begin{bmatrix} I & 0 \end{bmatrix} \quad (10)$$

In order to satisfy Eq. (10), $T_{11} = I$ and $T_{12} = 0$. From Eq. (8), it is obvious that

$$\begin{bmatrix} 0 & I \\ A_{21} & A_{22} \end{bmatrix} \begin{bmatrix} I & 0 \\ T_{21} & T_{22} \end{bmatrix} = \begin{bmatrix} I & 0 \\ T_{21} & T_{22} \end{bmatrix} \begin{bmatrix} (\tilde{A})_{11} & (\tilde{A})_{12} \\ (\tilde{A})_{21} & (\tilde{A})_{22} \end{bmatrix} \quad (11)$$

which produces $T_{21} = (\tilde{A})_{11}$, and $T_{22} = (\tilde{A})_{12}$. Thus, the transformation matrix $T$ that transforms $(\tilde{A}, \tilde{B}, \tilde{C})$ to $(A, B, C)$ in physical coordinate becomes

$$T = \begin{bmatrix} I & 0 \\ (\tilde{A})_{11} & (\tilde{A})_{12} \end{bmatrix} \quad (12)$$

After the transformation is completed, it is easy to find $H_{i=1...3}$ that are simply the partitions of $A, B$ as

$$H_1 = -A_{21}, \qquad H_2 = -A_{22}, \qquad H_3 = B_2 \quad (13)$$

### 2.2 Extracting system matrices

Having rearranged a realized state-space model $(A_r, B_r, C_r)$ into a physical coordinate system

$(A, B, C)$ through two consecutive transformations ($Q, T$), all partitions $H_{i=1...3}$ are defined. Next, physical parameters of second-order dynamical system ($M, \Theta$, and $K$) can be simultaneously recovered with the aid of the Kronecker product ($\otimes$) and the stack operator ($(\ )^s$). The following identity is used [13].

$$(ABC)^S = (C^T \otimes A)B^S \qquad (14)$$

In order to maintain the symmetry of $M, K$, and possibly $\Theta$, two additional equations should be considered as

$$\begin{aligned} MH_1 &= H_1^T M \\ MH_2 &= H_2^T M \end{aligned} \qquad (15)$$

Imposing symmetry conditions in Eq. (15) plays a key role in finding $M, K$, and $\Theta$ because knowing $H_{i=1...3}$ is not enough to solve Eq. (15). Also, note that the symmetry condition of the damping matrix ($\Theta$) is not needed for the case of non-symmetric damping. Combining Eqs. (5) and (15), we have the following set of linear equations:

$$\begin{aligned} K^S &= (H_1^T \otimes I)M^S \\ \Theta^S &= (H_2^T \otimes I)M^S \\ B^S &= (H_3^T \otimes I)M^S \\ (H_1^T \otimes I)M^S &= (I \otimes H_1^T)M^S \\ (H_2^T \otimes I)M^S &= (I \otimes H_2^T)M^S \end{aligned} \qquad (16)$$

Thus, the elements of mass, stiffness, and damping matrices are determined by solving a linear equation,

$$RP = S \qquad (17)$$

where

$$R = \begin{bmatrix} H_1^T \otimes I & 0 & -I \\ H_2^T \otimes I & -I & 0 \\ H_3^T \otimes I & 0 & 0 \\ (H_1^T \otimes I) - (I \otimes H_1^T) & 0 & 0 \\ (H_2^T \otimes I) - (I \otimes H_2^T) & 0 & 0 \end{bmatrix},$$

$$P = \begin{bmatrix} M^S \\ \Theta^S \\ K^S \end{bmatrix}, \quad S = \begin{bmatrix} 0 \\ 0 \\ B^S \\ 0 \\ 0 \end{bmatrix} \qquad (18)$$

As long as $R$ is full (column) rank, the symmetry condition on the damping matrix is not needed to solve for the elements of $M, K$, and $\Theta$ because Eq. (18) actually contains more equations than the minimum needed [11].

## 3. Experimental procedure

### 3.1 Description of torsional system

As described in reference [12], originally the torsional system has three inertia disks connected by two torsionally flexible rods or preferably called torsional springs [14]. By clamping the top disk to the body frame, a 2-DOF spring-mass-damper system of fixed-free boundary condition can be modeled as shown in Fig. 1. The brushless servo motor, as an input force, drives the shaft that is linked to the bottom disk by torque $T(t)$. The angular displacement ($\theta$) of each disk is measured from an optical encoder attached through a rigid belt and pulley. Therefore, the test structure in this study has a single torque input and two angular displacement outputs.

As shown in Fig. 1, the stiffness of the torsional spring or rod and the inertia of disk are defined as $k_i$ and $J_i$, respectively. We assume that placing a stiffener-type clamp at the center of a torsional spring rod creates stiffness changes. This clamp locally resists the rotation of the rod so that the stiffness of the tor-
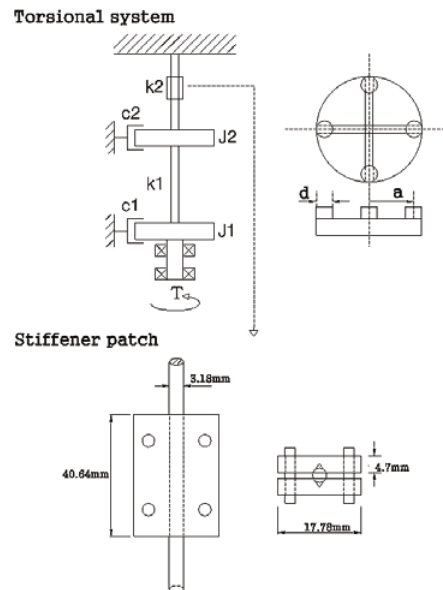


Fig. 1 Schematics of 2-DOF torsional system: assembly and stiffener patch for stiffness damage.

sional spring is increased by a certain degree. The degree of stiffening is a nonlinear function of the contact force and the area between the spring rod and the stiffening plate. Mass damage is also easily implemented by relocating mass blocks on each disk. As shown in Fig. 1, each disk has four mass blocks and adjustable slots. The inertia of the disk can be roughly estimated from calculating the mass of four blocks and their distance to the centerline ( *a* ). Thus, both stiffness and inertia of torsional system can be readily perturbed to imitate different types of damage conditions.

### 3.2 Identification of state-space model

A Gaussian random noise input to the servo motor excites the torsional system for 60 seconds having sampling time of 0.01 second. Also, dSPACE software has been used for data acquisition. Then, state-space system matrices are sought from the input/output time history data by using the OKID-ERA. A comparison between the experimental response and the predicted response of an identified state-space model from OKID-ERA is presented in Fig. 2 and Fig. 3. For verification, only the first half of the 60 sec. input-output data record was used in the identification, and the identified model is checked against the second half of the input-output data record. Note that only the last 5 seconds out of total 60-second sample are illustrated for comparison. To capture the true dynamics of the torsional system, different values of parameter $p$ in the OKID algorithm have been used [6]. The $p$ is related to the number of non-zero observer Markov parameters, which also represents the upper bound on the order of the identified system model. Fig. 2 and Fig. 3 provide results for $p = 2$, and $p = 20$, respectively. It is obvious that $p = 2$ exhibits a nearly similar prediction of experiment data compared to the case of $p = 20$. Several other values of $p$, greater than 20, have been tried for verification. Since values of $p$ greater than 20 do not give much improvement in prediction accuracy, hereafter a fixed value of $p = 20$ is used for all identification experiments. The final order of the identified model has been reduced to four ($n = 4$) through the singular value spectrum of the Hankel matrix. Having determined the minimal state-space model, the stiffness and mass matrices of the system are going to be extracted through the KP method. Note that this transformation requires the number of measurement outputs to be equal to the DOFs of a second-order model,
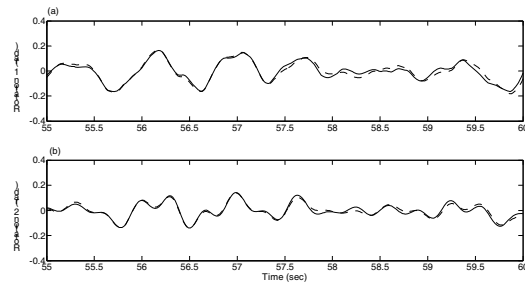


Fig. 2. Comparison between experiment ( … ) vs. OKID predicted simulation (—) with *p*=2, upper (a): angular rotation of disk 1, lower (b): angular rotation of disk 2

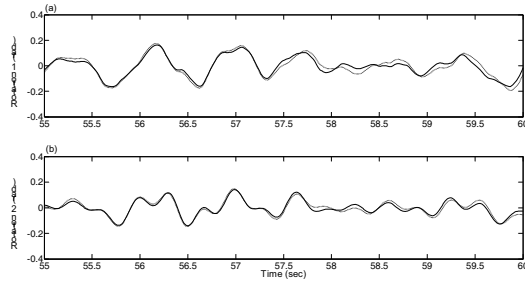

Fig. 3. Comparison between experiment (…) vs. OKID predicted simulation (—) with *p*=20, upper (a): angular rotation of disk 1, lower (b): angular rotation of disk 2.

a condition that is satisfied by encoder for measuring rotational angle at each disk. In other words, the number of measurements determines the size of stiffness and mass matrices.

### 3.3 Identification of structural parameters

To represent the dynamics of a torsional system, the friction caused from support bearings is idealized to viscous damping ( $c_i$ ) on each disk. Thus, the equation of motion is

$$\mathsf{J}\ddot{\theta}(t) + \Theta\dot{\theta}(t) + \mathsf{K}\theta(t) = \mathsf{B}u(t) \qquad (19)$$

where $\mathsf{J}, \Theta$ , and $\mathsf{K}$ are mass moment of inertia, damping, and stiffness matrices, respectively:

$$\mathsf{J} = \begin{bmatrix} J_1 & 0 \\ 0 & J_2 \end{bmatrix}, \ \Theta = \begin{bmatrix} c_1 & 0 \\ 0 & c_2 \end{bmatrix}, \ \mathsf{K} = \begin{bmatrix} k_1 & -k_1 \\ -k_1 & k_1 + k_2 \end{bmatrix} \qquad (20)$$

Here, input $\mathsf{B}u(t)$ represents a torque, $T(t)$ , applied on disk 1 from the servo motor. $\theta(t) = \begin{bmatrix} \theta_1 & \theta_2 \end{bmatrix}^T$ are angular positions of lower and upper disk in Fig. 1, respectively. Transforming this

into state-space form,

$$\dot{x} = Ax + Bu \tag{21}$$

where,

$$A = \begin{bmatrix} 0 & I \\ -J^{-1}K & -J^{-1}\Theta \end{bmatrix}, \quad B = \begin{bmatrix} 0 \\ J^{-1}B \end{bmatrix} \tag{22}$$

and the state is $x = \begin{bmatrix} \theta & \dot{\theta} \end{bmatrix}^T$. Since, a state-space model $(A_r, B_r, C_r)$ is identified from OKID-ERA, discrete second-order system matrices $(J, \Theta, K)$ are now to be reconstructed by KP method. The serial process from OKID, ERA, and KP is conveniently denoted as OKID-ERA-KP hereinafter.

Fig. 4 shows a histogram of experimentally identified structural parameters of a healthy state: mass moment of inertia ($J_i$), stiffness ($k_i$), and damping ($c_i$), $i = 1, 2$. The experiments for identification have been repeated 100 times over several days in order to get a reasonable statistical distribution for each individual parameter. The thin line in the histogram indicates the mean value of the parameter. The standard deviations of each parameter, as a percent of mean value for 100 trials, are $J_1 = 0.32\%$, $J_2 = 0.41\%$,

$k_1 = 0.43\%$, $k_2 = 0.57\%$, $c_1 = 0.84\%$, and $c_2 = 0.65\%$. The identified inertia ($J_i$) and stiffness ($k_i$) parameters are considered as relatively stable, while viscous damping ($c_i$) seems more easily affected by environmental conditions such as temperature, humidity or experimental hardware setup. Fig. 5 shows a comparison between system parameters identified through the proposed OKID-ERA-KP method and nominal values from manufacturer's specifications [14]. While, the '+' indicates the identified value of a system parameter from OKID-ERA-KP, the thin line shows the nominal value. The OKID-ERA-KP method generally gives a consistent identification with reference to nominal parameter values. It is not easy to identify absolute values of each system parameter as is assembled. There exist experimental uncertainties such as misalignment of rods, nonlinear friction, and unknown mass of the disk itself. Moreover, the relative deviation from healthy state is more important than the absolute value of the parameter if diagnosis is the main goal of this structural health monitoring scheme. The connection between a pulley and a belt from a servo motor produces significant amount of nonlinear damping which is difficult to approximate as linear damping. Because the main focus of this experiment
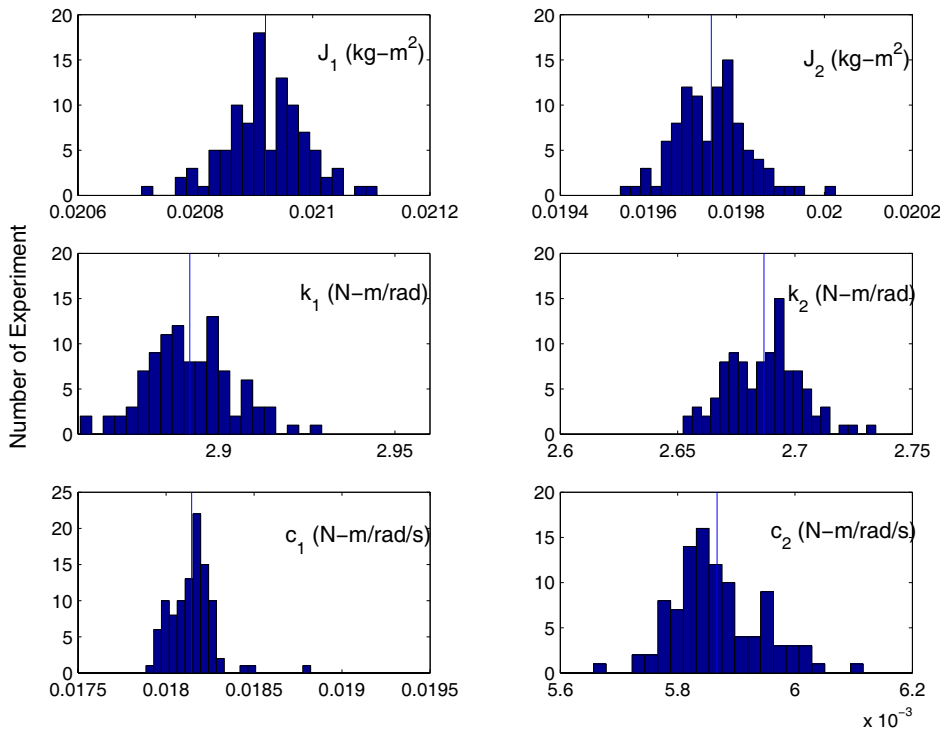


Fig. 4. Histogram of OKID-ERA-KP identified system parameters of torsional system model: thin line indicates a mean value.
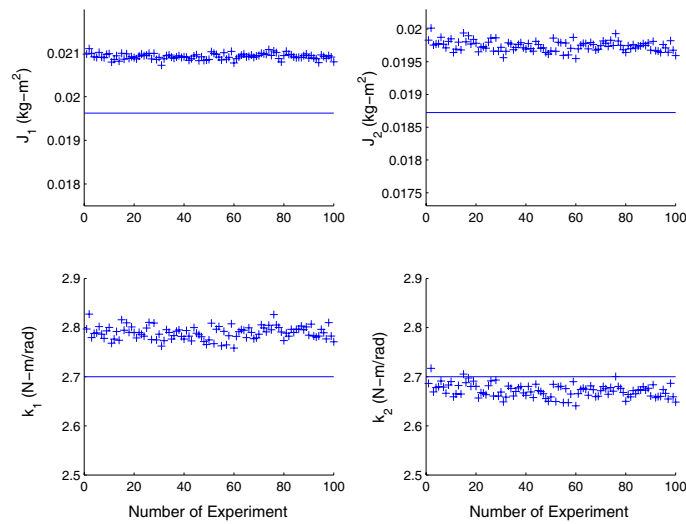
Fig. 5. Comparison between identified system parameters of torsional system: '+': OKID-ERA-KP method, '—': nominal values.
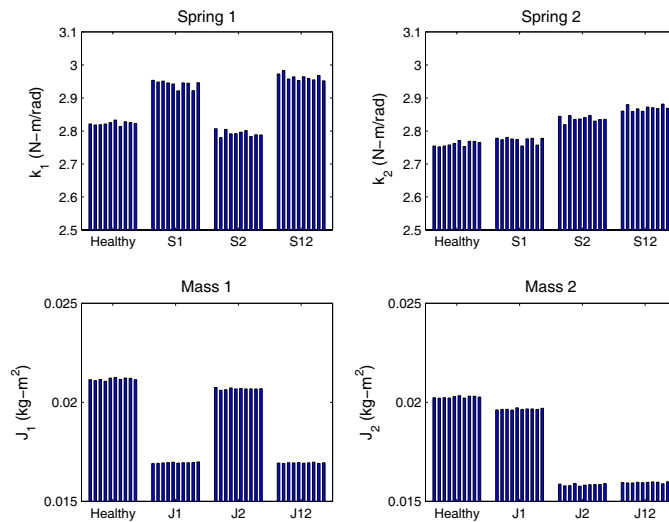


Fig. 6. Experimentally identified stiffness and mass moment of inertia for healthy and six different damage cases: *S1, S2, S12, J1, J2,* and *J12*.

lies in the change of mass and stiffness, the identified damping parameters are not significantly considered here.

## 4. Damage cases and experiment results

In total, nine different damage cases are investigated. The first three belong to mass damage: two for mass change on each individual disk and the other one for dual damage on both disks. Here, mass damage is created by moving four mass blocks ($4 \times 0.5$ kg) by 10*mm* toward the center of the disk so that the

total inertia for each disk is reduced by approximately 18%. Similar to mass damage, three different stiffness damages are generated: two cases for each individual torsional spring and the other one for dual damages on both springs. In case of stiffness damage, unlike mass, the true magnitude of stiffness change is not known *a priori*, as it depends on nonlinear contact characteristics between the clamp and the rod. Finally, the last three cases consider a group of mixed type damages such as simultaneously occurring damages on both spring rod and disk. This mixed type damage will illustrate the advantage of the proposed method

over other modal-based damage detection approaches that only use modal frequency change.

Fig. 6 illustrates identified stiffness and mass parameters of the torsional system for healthy and six different damage cases: (*S1*) stiffness damage on spring 1 ($k_1$), (S2) stiffness damage on spring 2 ($k_2$), and (*S12*) for dual damage on both springs. Likewise, mass damage on the disk is denoted as *J1*, *J2*, and *J12*. The individual experiment of healthy and damage cases has been repeated 10 times. The height of a bar indicates the identified value of the system parameters: the spring stiffness and mass inertia of the disk. It is obvious from the figure that stiffness changes are observed between healthy and each damage case. Since stiffness damage in this experiment is caused by a stiffener patch, spring constants are actually increased compared to healthy cases. The first plot in the figure (*Spring 1*) clearly shows the stiffness increment on the damage cases *S1* and *S12* compared to *Healthy* and S2. Likewise, in the case of *Spring 2*, damage *S2* and *S12* get higher spring constant values than those of *Healthy* and *S1* cases, which clearly indicates a distinction between damaged and healthy states. Especially, differences between healthy and damaged states of mass (*Mass 1* and *Mass 2*) are more significant than the stiffness case. Note that mass damage produces a consistent mass reduction ratio of 20%, which is very close to the true reduction of mass moment of inertia (18%). In general, identifying mass change is more accurate than identifying stiffness change. From the perspective of the experi-

ment, implementing mass perturbation on the disk is easier than increasing stiffness of the spring. Also, attaching a stiffener may produce a similar effect of nonlinear damping to the whole system. Table 1 summarizes the mean values of identified stiffness, mass, and damping parameters for all cases.

Fig. 7 presents identification results for mixed-type damage cases. Here, it is considered that two different types of damages, stiffness and mass damages, are occurring simultaneously. For example, the damage case *S2J1* denotes stiffness damage on spring 2 and mass damage on disk 1. Again, the true severities of stiffness damage are unknown in advance. The identified stiffness and mass parameters clearly indicate that variations of parameter are individually identified regardless of other damage types. For instance, *S1J1* increases the stiffness value of spring 1 alone, while *S2J2* only reduces the inertia for mass 2. Thus, identi-

Table 1. Experimentally identified stiffness $k_i$, mass $J_i$, and damping $c_i$ for healthy and damaged cases (all in suitable units). The bold number indicates the identified parameters of damaged one.

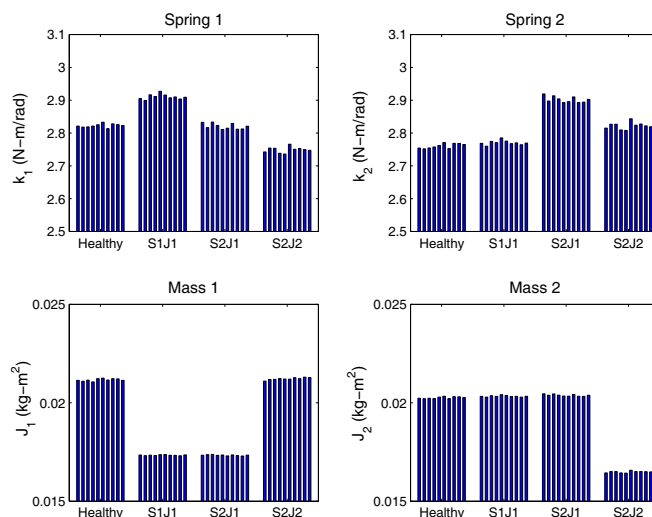| Parameters | Healthy | Damage Cases | | | |
|---|---|---|---|---|---|
| | | *S1* | *S2* | *J1* | *J2* |
| $k_1$ | 2.8228 | **2.9421** | 2.7931 | 2.7350 | 2.7022 |
| $k_2$ | 2.7606 | 2.7726 | **2.8369** | 2.6631 | 2.5940 |
| $J_1$ | 0.0212 | 0.0212 | 0.0211 | **0.0169** | 0.0207 |
| $J_2$ | 0.0203 | 0.0203 | 0.0200 | 0.0197 | **0.0158** |
| $c_1$ | 0.0163 | 0.0156 | 0.0159 | 0.0138 | 0.0167 |
| $c_2$ | 0.0062 | 0.0065 | 0.0068 | 0.0069 | 0.0059 |



Fig. 7. Experimentally identified stiffness and mass moment of inertia for healthy and three mixed damage cases: *S1J1, S2J1,* and *S2J2*.
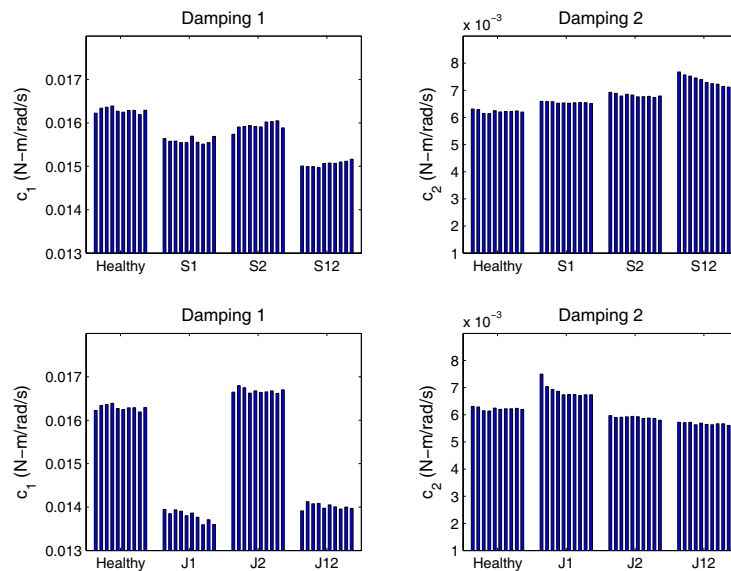
Fig. 8. Experimentally identified damping parameters for healthy and six different damage cases: *S1, S2, S12, J1, J2,* and *J12.*

fication of each parameter is not affected by the presence of different types of damage. Similar to the result of the homogeneous damage case (Fig. 6), the identified mass parameters are more consistent than the stiffness parameters.

It is well known that mass and stiffness changes associated with certain extent and location may produce no natural frequency shift at all due to canceling effects, which makes it difficult to detect damage by using only frequency-domain measurements. Thus, direct reconstruction of stiffness and mass matrices has an advantage over other modal-based methods, especially when the type of damage is unknown. In this regard, the torsional plant provides a perfect exemplary apparatus for demonstrating damage detection capability, i.e., differentiating damage types in a structure. The torsional system can accommodate various types and conditions of parameter perturbations without imposing interference between them. This experiment shows that mass and stiffness can be independently identified regardless of location and amount of their changes. The identified damping parameters exhibit somewhat contrasting results. The damping parameters are not significantly affected by stiffness and mass changes except for the *Damping 1* in the mass damage cases (*J1*, *J2*, and *J12*), as shown in Fig. 8. While damping is not generally considered as a damage-sensitive parameter, it is obvious that damping is more closely coupled with mass change in

this experiment.

## 5. Conclusions

This experimental study has shown that direct identification of stiffness and mass matrices from input-output data provides a potential tool for structural damage detection. The aforementioned approach does not require initial finite element models or frequency-domain data. The method offers a linear solution in extracting mass, damping and stiffness matrices from realized state-space models without solving an eigenvalue problem. This experimental validation of KP method allows us to envision potential solutions for more general inverse vibration problems. The significance of this study can be found in the experimental application of newly developed system identification techniques to practical problems of structural health monitoring without given prior information of a structure. Although the test structure belongs to a simple representation of a lumped mass system, the location, extent, and types of structural changes can be successfully identified. At the present, this technique can only reconstruct structural matrices of a system having all degree-of-freedoms measurable. However, the true dimension of a real structure is infinite, while the number of measurable states is limited. Thus, the challenge is to make an identified dynamics of the structure fit into a smaller dimensional space while

preserving the physical nature of the system. This type of problem is categorized as a reduced-order modeling [15, 16]. A high fidelity, reduced-order-model will alleviate errors caused by dimensional discrepancy in system identification. The issues regarding reduced-order modeling are still underway and will be addressed in future work.

## Acknowledgments

The authors wish to thank Prof. Laura Ray for helpful discussions on the use of the experiment data reported in this paper.

## References

[1] P. C. Chang and A. Flatau, Health monitoring of civil structures, in Proceedings of the First European Workshop on Structural Health Monitoring, Paris, France, 2002, 21-30.

[2] J. E. Mottershead and M. I. Friswell, Model updating in structural dynamics: A survey, Journal of Sound and Vibration, 165 (2) (1993) 347-375.

[3] H. G. Natke, Problems of model updating procedures: A perspective resumption, Mechanical Systems and Signal Processing. 12 (2) (1998) 65-74.

[4] M. I. Friswell and J. E. T. Penny, The practical limits of damage detection and location using vibration data, in Proceedings of the 11th VPI & SU Symposium on Structural Dynamics and Control, Blacksburg, Virginia, (1997) 31-40.

[5] J.-T. Kim and N. Stubbs, Model-Uncertainty Impact and Damage Detection Accuracy in Plate Girder, Journal of Structural Engineering, October, (1995) 1409-1417.

[6] J.-N. Juang, M. Q. Phan, L. G. Horta and R. W. Longman, Identification of Observer/Kalman Filter Markov parameters: Theory and experiments, Journal of Guidance, Control, and Dynamics. 16 (2) (1993) 320-329.

[7] J.-N. Juang and R. S. Pappa, An eigensystem realization algorithm for model parameter identification and model reduction, Journal of Guidance, Control, and Dynamics, 8 (5) (1985) 620-627.

[8] K. F. Alvin and K. C. Park, Second-order structural identification procedure via state-space-based system identification, AIAA Journal. 32 (2) (1994) 397-406.

[9] D. H. Tseng, R. W. Longman and J.-N. Juang, Identification of gyroscopic and nongyroscopic second-order mechanical systems including repeated roots problems, Advances in Astronautical Sciences. 87 (AAS 94-151) (1994) 145-165.

[10] D. Angelis, H. Lus, R. Betti and R. W. Longman, Extracting physical parameters of mechanical models from identified state space representations, ASME Journal of Applied Mechanics. 69 September (2002) 617-625.

[11] M. Q. Phan and R. W. Longman, Extracting mass, stiffness, and damping matrices from identified state-space models, Paper AIAA-2004-5415, AIAA Conference on Guidance, Navigation, and Control, Providence, RI, August 16-19, 2004.

[12] L. R. Ray and B. H. Koh, Enhancing Uniqueness Properties in Damage Identification using Sensitivity Enhancing Control, Materials Evaluation. 61 (10) (2003) 1134-1142.

[13] A. Graham, Kronecker products and matrix calculus with applications, Halsted Press, Horwood, New York, 1981.

[14] T. R. Parks, Manual for Model 205/205a: Torsional Control System, EPC Educational Control Products, Woodland Hills, California, 91367, (1999).

[15] K. F. Alvin, L. D. Peterson and K. C. Park, Method for Determining Minimum-Order Mass and Stiffness Matrices from Modal Test Data, AIAA Journal. 33 (1) (1995) 128-135.

[16] J. Yu, M. De Angelis, M. Imbimbo and R. Betti, Damage Detection in Reduced Order Models of Linear Structural Systems, Proceedings of the 4th International Workshop on Structural Health Monitoring. (2003) 403-410.